

COMPARISON OF FUSION SCHEMES FOR TWO-VIEW ANALYSIS OF BREAST CANCER USING MAMMOGRAMS

Lavanya R., Department of Electronics and Communication Engineering, Amrita School of Engineering, Amrita Vishwa Vidyapeetham, Amritanagar, Coimbatore-641 112, India; Nagarajan N., Department of Computer Science and Engineering, Coimbatore Institute of Engineering and Technology, Narasipuram, Coimbatore-641 109, India.

Abstract

Recently, integration of information from multiple sources is gaining wide popularity in data analysis. In developing computer aided diagnosis (CADx) systems for breast cancer, information fusion from the two standard mammographic views would serve to mimic the radiologist's practice of analyzing these two views in combination. In this work, different fusion strategies are used to realize two-view CADx systems for classification of breast masses. Two different databases are used for validation. One of the databases is a publicly available database called the digital database of screening mammography (DDSM) and the other one is a private database. The results demonstrate that the performance of a particular fusion strategy depends on the dataset under consideration. Further, it is not possible to predict the behavior of these fusion strategies before actually testing them. Thus, employing an arbitrary benchmark fusion strategy for building a two-view CADx system may not guarantee the best performance improvement when compared to single-view systems. This leads to the conclusion that a systematic approach is necessary prior to fusion to suitably transform the datasets under consideration so as to optimize fusion in a two-view CADx framework.

Introduction

Breast cancer is the primary cause of death due to cancer in women. Detecting breast cancer in early stages can prevent mortality without the need for mastectomy. Mammography is the most effective and commonly used imaging modality for screening breast cancer in asymptomatic women. It has been shown that mammographic screening is effective in reducing breast cancer mortality rates. However, the factors that limit the performance of radiologists in interpreting mammograms are the subtle nature of abnormalities and complexity of the breast tissue. Double reading by two different radiologists has been opted to overcome this problem. However, the process is time consuming and may result in ambiguous diagnostic decisions [1].

Computer aided detection/diagnosis (CADE/CADx) systems assess breast images objectively as opposed to the sub-

jective analysis made by the radiologists [3aece]. While CADE systems determine suspicious regions in mammograms, CADx systems are used for classifying the abnormal regions as benign or malignant [2]. Accurate classification of breast abnormalities is a crucial task. Due to the low specificity of mammograms, the number of benign cases that have been misinterpreted as malignant and hence subjected to biopsy has been very high. This results in unnecessary physical, emotional and financial discomfort to the patients. Many studies show that the use of a CAD system as a second reader can help radiologists in improving the accuracy of breast cancer detection and diagnosis [3].

A routine mammographic examination involves recording two standard views of the breast. These are the mediolateral (MLO) view, which is a side-to-side view and the craniocaudal (CC) view, which is a head-to-toe view. Radiologists usually read both views simultaneously to arrive at a decision. Bassett et al. [4] compared single view and two-view mammographic examinations which were interpreted by experienced radiologists. The authors reported that the number of call-back examinations reduced with two-view examinations. Blanks et al. [5] and Hackshaw et al. [6] analyzed the impact of two-view examinations on mammographic screening and reported that it improved the cancer detection rate.

Motivated by this, several researchers have worked towards the development of CADx systems using two mammographic views for classification of microcalcification clusters (MCCs) [7], [8], [9] and masses [10], [11] as benign or malignant. All these CADx systems have employed different decision-level and/or feature-level fusion strategies to combine information from the two views. Various fusion strategies employed in state-of-the art two-view CADx systems are listed in Table 1. Decision fusion involves merging of local decisions based on individual sources. Decision level fusion may be either soft decision fusion (centralized data fusion) or hard decision fusion (distributed decision fusion). In the former, information is derived from multiple feature sets and integrated directly into a final decision. In the latter, the individual decisions are first derived based on different feature sets and then combined into a global decision. On the other hand, feature fusion involves extraction of features

from different data sources followed by merging of these feature sets [12]. Decision level fusion may be either soft decision fusion (centralized data fusion) or hard decision fusion (distributed decision fusion). In the former, the individual decisions are first derived based on different feature sets and then combined into a global decision. In the latter, information is derived from multiple feature sets and integrated directly into a final decision [13]. Decision fusion is advantageous when multiple sources of information are uncorrelated, whereas feature fusion is appropriate when the sources are correlated [12]. However, due to the fact that different sources of information usually have correlated and uncorrelated components, these fusion strategies are sub-optimal. This means that the dataset involved in the training process solely determines the performance improvement that can be achieved by a given fusion technique over the single-view systems. No single fusion technique is guaranteed to yield superior performance consistently and universally. This fact has been demonstrated in this work in the context of classification of masses. This is an especially challenging task due to wide range in size, shape and contrast of masses [14]. Typically, benign masses are round or oval in shape and have a well-circumscribed boundary; on the other hand, malignant masses are characterized by irregular shape and spiculated boundary. Nevertheless, in many instances equivocal cases might be encountered. Examples include spiculated benign masses and well-circumscribed malignant tumors [15].

In this work, the performances of single-view CADx systems and two-view CADx systems based on different benchmark fusion strategies have been compared using two different databases. In section 2, the materials and methods used in the work have been described. In Section 3, the results and discussion have been presented. In section 4, the conclusion and future directions have been provided.

Materials and Methods

The flow of the work is shown in Fig. 1. The details of the two databases used in this work are as follows. The first one is a widely used public database called the digital database for screening mammography (DDSM) from the University of South Florida [16]. A total of 104 pairs of MLO and corresponding CC images are used for the study, out of which 36 are benign and 68 are malignant. The other database used is a private database comprising 53 pairs of MLO and CC images collected from a private hospital. Out of these images, 37 are benign and 16 are malignant. In the DDSM database, radiologists have described and assessed suspicious masses using breast image-reporting and data system (BI-RADS) descriptors. In the private database, the ground truth related to diagnostic findings and nature of the masses have been provided by expert radiologists.

Table 1. Fusion Techniques Used in Existing Work

S.No.	Approach	Level of fusion
1	Maximum rule [7], [10], [11]	Soft decision fusion
2	Minimum rule [10], [11]	Soft decision fusion
3	Sum rule [7], [8], [10], [11]	Soft decision fusion
4	Product rule [11]	Soft decision fusion
5	Linear discriminate Analysis (LDA) [11]	Soft decision fusion
6	OR rule [9]	Hard decision fusion
7	Serial [9], [11]	Feature fusion
8	Parallel [9], [11]	Feature fusion

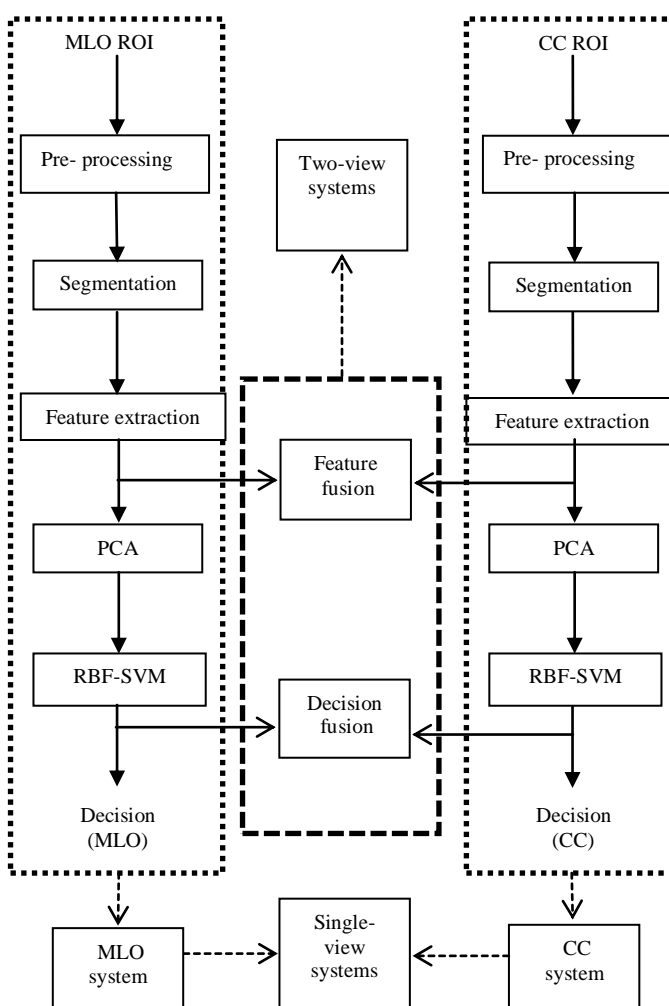


Figure 1. Schematic of the work flow
A. Image Processing

Prior to employing information fusion, MLO and CC images in each database are cropped to regions of interest

(ROIs) containing mass regions marked by the radiologists. The cropped ROIs are then subjected to pre-processing followed by segmentation of masses and feature extraction.

(I) Pre-processing

Mammograms are predominantly affected by quantum noise which results in poor resolution of the acquired image. Hence denoising is an essential step in processing a mammogram. Further, the subtle nature of lesions and the low contrast of mammograms necessitates enhancement of mammograms prior to segmentation. Denoising and subsequent enhancement of mammographic images could improve the accuracy of detection of early signs of breast cancer [1], [14]. In this work, two-dimensional (2D) median filter with a 3×3 mask is employed for denoising the ROIs. A median filter is an order-statistic, non-linear smoothing filter which ranks the pixels of the image area encompassed by the filter and replaces the center pixel value of the image by the value determined by the ranking result [17]. The ROIs are subjected to contrast limited adaptive histogram equalization (CLAHE) for enhancement. In adaptive histogram equalization (AHE), a pixel’s intensity is transformed to a value proportional to the pixel intensity’s rank in the histogram of a local region. CLAHE differs from AHE in that a user-specified maximum is imposed on the height of the local histogram so as to reduce over-enhancement of noise and edge shadowing effect [18].

(II) Segmentation

Detection of masses in a mammogram is a non-trivial task due to the complex nature of the breast tissue. The difficulty of segmentation increases for early lesions and/or dense tissues. An adaptive thresholding algorithm [19] based on wavelet analysis is used to perform segmentation of masses in the ROIs. First, the preprocessed image is subjected to a two-stage Daubechies-10 (Daub-10) wavelet transform. A coarse segmentation using histogram-based adaptive global thresholding is performed on the LL sub-band obtained as a result of first stage wavelet analysis of the mammogram image. Morphological enhancement of the LL sub-band obtained after the second stage of wavelet decomposition is performed using tophat filtering. The coarse segmented output and the outcome of morphological enhancement are combined using convolution. Following this, finer segmentation is performed using a window-based adaptive local thresholding on the combined result to yield the final segmented output. Here, the role of coarse segmentation is to yield a rough representation of the suspicious region’s location. This is further improved upon by the finer segmentation to yield more precise results. Original images of a sample ipsilateral mammogram pair, the manually cropped ROIs and the corresponding segmented outputs are shown in Fig. 2 for the DDSM database and Fig. 3 for the private database.

(III) Feature Extraction

To distinguish a malignant mass from a benign one, the internal luminance structure as well as the geometry of the mass is important. Texture features represent the luminance characteristics of a mass, whereas shape features reflect its

geometrical characteristics. A total of 33 features [20], [21], [22] listed in Table 2, comprising 14 texture features ($f_1 - f_{14}$) and 19 shape features ($f_{15} - f_{33}$) are extracted from the segmented masses. The texture features f_2 through f_{14} , called Haralick’s features are computed from gray-level co-occurrence matrix (GLCM) which is a measure of the spatial relationship of the gray levels in a mass. The remaining texture and shape features are calculated directly from the mass.

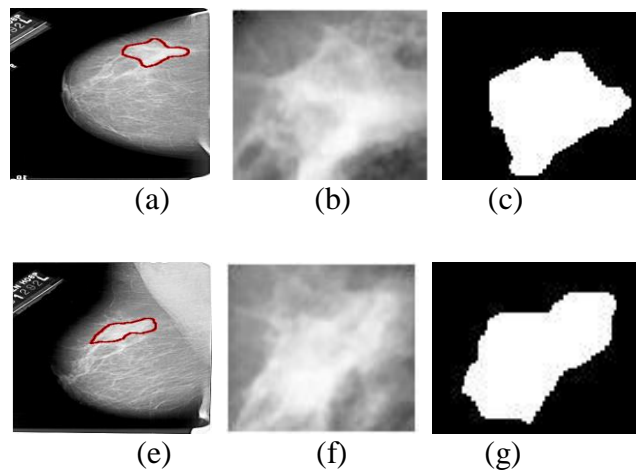


Figure 2. DDSM database: (a) Original MLO image, (b) MLO ROI, (c) Segmented output for MLO, (d) Original CC image, (e) CC ROI, and (f) Segmented output for CC

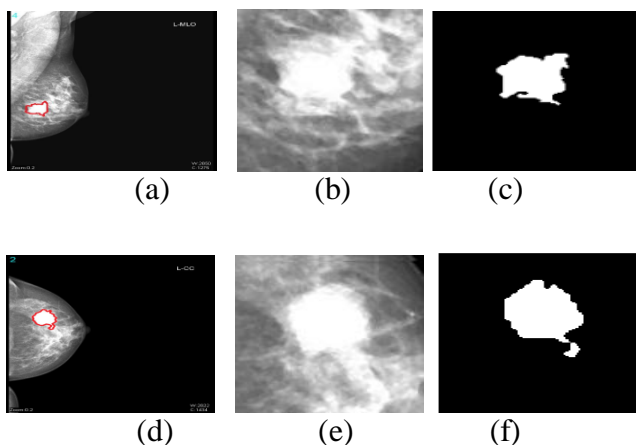


Figure 3. Private database: (a) Original MLO image, (b) MLO ROI, (c) Segmented output for MLO, (d) Original CC image, (e) CC ROI, and (f) Segmented output for CC

Table 2. List of Shape and Texture Features

Texture features	Shape features
f_1 :Entropy of the segmented mass	f_{15} :Area
f_2 :Contrast	f_{16} :Perimeter
f_3 :Correlation	f_{17} :Mean radius
f_4 :Angular second moment	f_{18} :Standard deviation of radius

f_5 :Entropy	f_{19} :Skewness of radius
f_6 :Sum of squares	f_{20} :Kurtosis of radius
f_7 :Sum average	f_{21} :Circularity
f_8 :Sum entropy	f_{22} :Roughness
f_9 :Sum variance	f_{23} :Long axis to short axis ratio
f_{10} :Difference entropy	f_{24} :Depth-to-width ratio
f_{11} :Difference variance	f_{25} :Zero-crossing
f_{12} :Inverse difference moment	f_{26} :Chain coding
f_{13}, f_{14} :Information measures of correlation	f_{27} - f_{33} :Hu's moments

B. Information fusion

Let $i = 1$ and $i = 2$ represent the MLO and CC sources, respectively. The raw feature vector f_i extracted from each of these sources is subjected to principal component analysis (PCA) for dimensionality reduction. The goal of PCA is to find a set of new attributes called principal components such that they are linear combinations of the original attributes, orthogonal to each other and capture the maximum amount of variation in the data. Often the variability of the data can be captured by a relatively small number of principal components and hence PCA can achieve high dimensionality reduction with usually lower noise than the original patterns. Each of the resulting reduced-dimension vector x_i is used to train a support vector machine (SVM) classifier separately. SVM is a supervised machine learning algorithm that is used for pattern recognition. Using a set of examples with known classes, SVM first builds a training model. This model is then used to predict the class of a new case. For building the model, SVM determines a separating hyperplane called maximum margin hyperplane such that the distance from the hyperplane to the closest training points on either side is maximized. In addition to performing linear classification, non-linear classification problems can also be efficiently solved by SVM. In such cases a non-linear transformation is used to map the data vector into a higher dimensional space where the data becomes linearly separable. SVM achieves this using a non-linear kernel function to perform the mapping implicitly. In this work, radial basis function (RBF) kernel is employed for this purpose. PCA and SVM have been widely used and shown to be effective for breast cancer diagnosis [23]. The outputs of each of the classifiers are the posterior probabilities $P(C_1/x_i)$, $P(C_2/x_i)$ and the hard decision D_i . Here, C_1 and C_2 represent the two classes, malignant and benign, respectively. In this way, single-view systems based on MLO and CC information are realized separately.

Following this, all fusion techniques employed in state-of-the-art two-view CADx systems listed in Table 1 are explored. Apart from these schemes, three additional fusion schemes, namely, weighted sum rule and weighted product rule (soft decision fusion schemes) and the AND rule (hard decision fusion) are also implemented. All these fusion

schemes are explained below in the context of combining an arbitrary number of sources, say, N . Letting $N = 2$ will make these fusion schemes appropriate for the problem under consideration for combining MLO and CC information.

(I) Soft Decision Fusion Schemes

These schemes make use of the posterior probability estimates of the single-source classifiers, to arrive at a final decision.

(i) Maximum rule

According to maximum rule, the final decision D_{max} , i.e., the class to which the input pattern is assigned is given by

$$(1). D_{max} = \arg \max_j \max_i P(C_j | x_i), i = 1..N; j = 1,2 (1)$$

(ii) Minimum rule

According to the minimum rule, the final decision D_{min} is defined as in (2).

$$D_{sum} = \arg \max_j \left(\frac{1}{N} \sum_{i=1}^N P(C_j | x_i) \right), j = 1,2 (2)$$

(iii) Sum rule

The final decision D_{sum} of the sum rule is given by (3).

$$D_{sum} = \arg \max_j \left(\frac{1}{N} \sum_{i=1}^N P(C_j | x_i) \right), j = 1,2 (3)$$

(iv) Weighted sum rule

This approach is a slight variation of the sum rule and the final decision D_{wsum} is determined by (4).

$$D_{wsum} = \arg \max_j \left(\sum_{i=1}^N w_i P(C_j | x_i) \right), j = 1,2 (4)$$

Here w_i is the weight associated with the i th classifier such

that $\sum_{i=1}^N w_i$ is equal to unity. The weighted sum rule is designed such that it can handle the imbalance in the accuracy of the classifiers. In this work w_i is chosen according to (5).

$$w_i = \frac{acc_i}{\sum_{i=1}^N acc_i}, i = 1..N (5)$$

Here acc_i is the validation accuracy of the N th classifier.

(v) Product rule:

According to the product rule, the final decision D_{prod} is expressed as in (6).

$$D_{prod} = \arg \max_j \left(\prod_{i=1}^N (P(C_j | x_i)) \right)^{\frac{1}{N}}, j = 1,2 (6)$$

(vi) Weighted product rule: This strategy is a modified version of the product rule with the final decision D_{wprod} being determined as in (7).

$$D_{wprod} = \arg \max_j \prod_{i=1}^N (P(C_j | x_i))^{w_i}, j = 1,2 (7)$$

Here also w_i is chosen according to (5).

(vii) LDA fusion:

In this fusion technique, the posterior probabilities of all the single source systems are concatenated to result in a vector f_{class} as given by (8).

$$f_{class} = [P(C_1 | x_1), P(C_1 | x_2), \dots, P(C_1 | x_N)] \quad (8)$$

This vector is given as input to a LDA classifier. The hard decision output of the LDA classifier for the input f_{class} is considered as the final decision D_{class} .

(II) Hard Decision Fusion Schemes

In these schemes, the hard decisions of single-source systems are used to arrive at the final decision.

(i) OR rule: In this approach, the final decision D_{or} is obtained by performing logical OR operation on the hard decisions as given by (9):

$$D_{or} = (D_1 \cup D_2 \dots \cup D_N) \quad (9)$$

(ii) AND rule: Here, the final decision D_{and} is arrived at by performing logical AND operation on the hard decisions and is given by (10):

$$D_{and} = (D_1 \cap D_2 \dots \cap D_N) \quad (10)$$

2.2.3. Feature Fusion Schemes

i) Serial fusion

In serial fusion, the raw feature vectors of all sources are concatenated to result in the feature vector f_{con} as shown in (11):

$$f_{con} = ([f_1, f_2, \dots, f_N]) \quad (11)$$

The concatenated vector f_{con} is then subjected to PCA for dimensionality reduction, resulting in the reduced vector x_{con} . This feature vector x_{con} is input to a RBF-SVM classifier, which outputs the hard decision D_{con} .

(ii) Parallel fusion

A feature vector f_{avg} is constructed by averaging MLO and CC features as given in (12):

$$f_{avg} = (f_1 + f_2 + \dots + f_N) / N \quad (12)$$

It is then subjected to PCA for dimensionality reduction, yielding x_{avg} . This feature vector x_{avg} is given as input to RBF-SVM classifier, which outputs the hard decision D_{avg} .

Results and discussion

For all the systems, a nested two-level, k-fold cross validation strategy (with $k = 10$) is employed, wherein the inner level is used for model selection and the outer level is used for performance evaluation. In k-fold cross-validation, the complete set of observations is randomly partitioned into k equal size subsamples. In each fold, $k-1$ groups are used for training and the remaining group for testing. This process is performed k times, such that each of the k groups is used exactly once for testing the model. As all the samples are involved in testing the model the estimation of the classifier performance is unbiased. While the testing is performed in

the outer level, validation is performed in the inner level, where the training set in each fold is subjected to a 10-fold cross validation for choosing the optimum parameters of the model for that fold. These free parameters include the SVM parameters c and γ as well as the number of principal components that are retained for dimensionality reduction. An exhaustive grid search is employed for parameter selection. The parameters that best capture the boundaries between the two classes of lesions are chosen as optimal parameters. During testing, the classifier is used to predict the labels of the independent test cases in each fold using the optimized parameters for the respective fold. The testing process is repeated for all 10 folds.

The area under the receiver operating curve (AUROC) is used as the metric for evaluating the performance of various systems. The receiver operating curve (ROC) is a plot of true positive rate (TPR) along the y-axis and false positive rate (FPR) along the x-axis for different decision thresholds in a binary decision problem, where TPR and FPR are given by (13) and (14), respectively:

$$TPR = Sensitivity = \frac{TP}{TN + FP} \quad (1)$$

$$FPR = 1 - Specificity = \frac{FP}{TN + FP} \quad (2)$$

An ideal ROC curve would start at (0,0), move vertically upward to (0,1) and then horizontally to (1, 1). The AUROC derived from the ROC plot is considered to be a good measure that summarizes the test accuracy. It can assume a value that ranges from 0 to 1. The closer its value is to 1, the better is the diagnostic performance of the test.

The AUROC is computed for various single-view and two-view (fusion-based) systems for the DDSM database as well as the private database. These values are tabulated in Table 3 for the DDSM database. It can be observed from Table 3 that all fusion schemes outperform the single-view systems in terms of AUROC. The parallel feature fusion scheme yields the best performance among all systems. It can be seen that this scheme outperforms the single-view systems by at least 6% and at most 8%. In Table 4, the AUROC values for the private database are compared. It can be observed from the table that all fusion schemes except the LDA fusion outperform both the single-view schemes. The LDA fusion performs better than only the MLO system and not the CC system. Also, unlike the DDSM database, the weighted sum rule demonstrates the best performance when compared to all other systems. The performance improvement of this scheme is observed to be at least 3% and at most 6% when compared to single-view systems.

Two observations are worth mentioning from the above analysis:

1) A fusion scheme which yields an improved performance when compared to single-view systems for one dataset need

not necessarily outperform single-view systems in the case of other datasets.

Table 2. Comparison of AUROC of Various Systems for the DDSM Database

System	AUROC
MLO	0.7403±0.0483
CC	0.7300±0.0492
Maximum rule	0.7410±0.0482
Minimum rule	0.7720±0.0454
Sum rule	0.7779±0.0448
Product rule	0.7846±0.0442
OR rule	0.7726±0.0454
AND rule	0.7846±0.0442
Weighted sum rule	0.7801±0.0446
Weighted product rule	0.7839±0.0442
LDA fusion	0.7488±0.0476
Serial fusion	0.7689±0.0457
Parallel fusion	0.7883±0.0438

Table 3. Comparison of AUROC of Various Systems for the Private Database

System	AUROC
MLO	0.7755±0.0757
CC	0.7487±0.0786
Maximum rule	0.7907±0.0738
Minimum rule	0.7795±0.0752
Sum rule	0.7952±0.0732
Product rule	0.7889±0.0740
OR rule	0.7963±0.0731
AND rule	0.7889±0.0740
Weighted sum rule	0.7974±0.0729
Weighted product rule	0.7931±0.0735
LDA fusion	0.7538±0.0781
Serial fusion	0.7856±0.0745
Parallel fusion	0.7967±0.0730
MLO	0.7755±0.0757

2) A fusion scheme that demonstrates the best performance when compared to single-view systems and other two-view systems for one dataset need not necessarily serve as the best for other datasets. Benchmark fusion techniques are thus sub-optimal and arbitrary choice of a particular fusion scheme might not yield the expected best performance.

Conclusion and Future Directions

The performance of several benchmark fusion schemes have been investigated for combining information from MLO and CC views of the mammogram for classification of masses. Two different databases (the publicly available DDSM database and another private database) have been involved for the comparative analysis. The analysis demonstrates that the performances of the schemes depend largely

on the dataset used and their behaviour cannot be predicted before they are actually tested on a given dataset. One possible direction in the search of an optimal fusion technique is to make use of the fact that feature fusion yields maximum benefit when the features to be fused are highly correlated. Thus a suitable transformation like canonical correlation analysis (CCA) that maximises the correlation between two multivariate datasets may be applied to the MLO and CC datasets prior to feature fusion. This technique has the potential to provide an optimal performance irrespective of the data to be fused.

References

- [1] J. Tang, R. M. Rangayyan, J. Xu, I. El Naqa and Y. Yang, "Computer-aided detection and diagnosis of breast cancer with mammography: recent advances," IEEE Transactions on Information Technology in Biomedicine, Vol. 13, No. 2, pp. 236-251, 2009.
- [2] A. Jalalian, S. B. Mashohor, H. R. Mahmud, M. I. B. Saripan, A. R. B. Ramli and B. Karasfi, "Computer-aided detection/diagnosis of breast cancer in mammography and ultrasound: a review," Clinical Imaging, Vol. 37, No. 3, pp. 420-426, 2013.
- [3] A. C. Bovik, Handbook of image and video processing. Academic Press, 2010.
- [4] L. W. Bassett, D. H. Bunnell, R. Jahanshahi, R. H. Gold, R. D. Arndt and J. Linsman, "Breast cancer detection: one versus two views," Radiology, Vol. 165, No. 1, pp. 95-97, 1987.
- [5] R. G. Blanks, M. G. Wallis, and R. M. Given-Wilson, "Observer variability in cancer detection during routine repeat (incident) mammographic screening in a study of two versus one view mammography," Journal of Medical Screening, Vol. 6, No. 3, pp. 152-158, 1999.
- [6] A. K. Hackshaw, N. J. Wald, M. J. Michell, S. Field, and A. R. M. Wilson, "An investigation into why two-view mammography is better than one-view in breast cancer screening," Clinical Radiology, Vol. 55, No. 6, pp. 454-458, 2000.
- [7] H. P. Chan, B. Sahiner, K. L. Lam, N. Petrick, M. A. Helvie, M. M. Goodsitt and D. D. Adler, "Computerized analysis of mammographic microcalcifications in morphological and texture feature spaces," Medical Physics, Vol. 25, No. 10, pp. 2007-2019, pp. 1998.
- [8] W. J. Veldkamp, N. Karssemeijer, J. D. Otten and J. H. Hendriks, "Automated classification of clustered microcalcifications into malignant and benign types," Medical Physics, Vol. 27, No. 11, pp. 2600-2608, 2000.
- [9] J. Wei, H. P. Chan, B. Sahiner, C. Zhou, L. M. Hadjiiski, M. A. Roubidoux and M. A. Helvie, "Computer-aided detection of breast masses on mammograms: Dual system approach with two-view

- analysis,” *Medical Physics*, Vol. 36, No. 10, pp. 4451-4460, 2009.
- [10] S. Gupta, P. F. Chyn and M. K. Markey, “Breast cancer CADx based on BI-RADS™ descriptors from two mammographic views,” *Medical Physics*, Vol. 33, No. 6, pp. 1810-1817, 2006.
- [11] S. Gupta, D. Zhang, M. P. Sampat and M. K. Markey, “Combining texture features from the MLO and CC views for mammographic CADx,” *SPIE Conference on Medical Imaging*, Vol. 61445, pp. 61445V-61445V9, March 2006
- [12] P. K. Atrey, M. A. Hossain, A. El Saddik and M. S. Kankanhalli, “Multimodal fusion for multimedia analysis: a survey,” *Multimedia Systems*, Vol. 16, No. 6, pp. 345-379, 2010.
- [13] J. Yang, J. Y. Yang, D. Zhang and J. F. Lu, “Feature fusion: parallel strategy vs. serial strategy,” *Pattern Recognition*, Vol. 36, No. 6, pp. 1369-1381, 2003.
- [14] N. H. Eltonsy, G. D. Tourassi and A. S. Elmaghraby, “A concentric morphology model for the detection of masses in mammography,” *IEEE Transactions on Medical Imaging*, Vol. 26, No. 6, pp. 880-889, 2007.
- [15] R. M. Rangayyan, F. J. Ayres and J. E. Leo Desautels, “A review of computer-aided diagnosis of breast cancer: Toward the detection of subtle signs,” *Journal of the Franklin Institute*, Vol. 344, No. 3, pp. 312-348, 2007.
- [16] M. Heath, K. Bowyer, D. Kopans, P. Kegelmeyer, R. Moore, K. Chang and S. Munishkumaran, “Current status of the digital database for screening mammography,” *Computational Imaging and Vision*, Vol. 13, pp. 457-460, 1998.
- [17] J. Nagi, S. Abdul Kareem, F. Nagi and S. K. Ahmed, “Automated breast profile segmentation for ROI detection using digital mammograms,” *IEEE EMBS Conference on Biomedical Engineering and Sciences* pp. 87-92, November 2010.
- [18] S. M. Pizer, E. P. Amburn, J. D. Austin, R. Cromartie, A. Geselowitz, T. Greer, B. M. ter Haar Romeny, J. B. Zimmerman and Zuiderveld, K. “Adaptive histogram equalization and its variations,” *Computer Vision, Graphics and Image Processing*, Vol. 39, No. 3, pp. 355-368, 1987.
- [19] K. Hu, X. Gao and F. Li, “Detection of suspicious lesions by adaptive thresholding based on multiresolution analysis in mammograms,” *IEEE Transactions on Instrumentation and Measurement*, Vol. 60, No. 2, pp. 462-472, 2011.
- [20] A. Mencattini, M. Salmeri, G. Rabottino and S. Salicone, “Metrological characterization of a CADx system for the classification of breast masses in mammograms” *IEEE Transactions on Instrumentation and Measurement*, Vol. 59, No. 11, pp. 2792-2799, 2010.
- [21] M. K. Hu, “Visual pattern recognition by moment invariants,” *IRE Transactions on Information Theory*, Vol. 8, No. 2, pp. 179-187, 1962.
- [22] H. Freeman, “On the encoding of arbitrary geometric configurations,” *IRE Transactions on Electronic Computers*, Vol. EC-10, No. 2, pp. 260-268, 1961.
- [23] H. D. Cheng, J. Shan, W. Ju, Y. Guo and L. Zhang, “Automated breast cancer detection and classification using ultrasound images: A survey,” *Pattern Recognition*, Vol. 43, No. 1, pp. 299-317, 2010.

Biographies

R. LAVANYA received the B.E. degree in Electronics and Communication Engineering from Bharathiar University, Coimbatore, Tamilnadu in 2001 and the M.E. in Applied Electronics from Anna University, Chennai, Tamilnadu in 2005. She is pursuing Ph.D. in the faculty of Information and Communication Engineering at Anna University, Chennai, Tamilnadu. She is an Assistant Professor of Electronics and Communication Engineering at Amrita School of Engineering, Amrita Vishwa Vidyapeetham. Her teaching and research areas include signal processing, biomedical image processing and soft computing. Professor R. Lavanya .

Dr. N. NAGARAJAN received the B.Tech and M.E. degrees in Electronics Engineering at M.I.T Chennai. He received his Ph. D. in the Faculty of Information and Communication Engineering from Anna University, Chennai. He is currently working as Principal in Coimbatore Institute of Engineering and Technology at Coimbatore. His teaching and research areas include optical, wireless and sensor networks. Professor N. Nagarajan .